ON SEDIMENT TRANSPORT RATES AND RELATED TIME SCALES FOR SAND BAR FORMATION IN COASTAL ZONES

by

Boczar-Karakiewicz, B. INRS-Océanologie, Université du Québec, 310 ave. des Ursulines, Rimouski, Québec, G5L 3A1

Bona, J.L. Department of Mathematics, The University of Chicago, 5734 University Ave, Chicago, IL 60637

Chapalain, G. Laboratoire d'Océanographie Physique, Université de Bretagne Occidentale, 6 Av. LeGorgeu, 29237 Brest, France

Abstract

Surface gravity waves in near shore shallow water and their interaction with bed topography are investigated. Such waves may deform sandy beds into systems of multiple shore-parallel bars. A mathematical model describing this interaction has been derived for normally incident progressive waves by postulating a viscous, laminar boundary layer near the bottom. Examined herein are variants of this model that use two more sophisticated descriptions of the near-bed boundary layer flows, one with the locally defined sediment concentration depending on the flow field, and the second following Bagnold-Bowen's «energetic» approach. Estimates of sediment transport rates and the related time scales of bed deformation are derived and calibrated using laboratory and field observations.

Résumé

Les houles en eau peu profonde et leur interaction avec le fond sont étudiées. Ces houles peuvent générer sur un fond sableux des systèmes de barres multiples parallèles à la côte. Un modèle mathématique décrivant cette interaction a été élaboré dans le cas d'une houle progressive d'incidence normale développant près du fond une couche limite laminaire. Des améliorations ont été apportées à ce modèle. Elles résultent de descriptions plus sophistiquées des caractéristiques de la couche limite de fond: l'une à partir d'une concentration locale dépendant de l'écoulement, l'autre reprenant l'approche «énergétique» de Bagnold-Bowen. Des estimations des taux de transport sédimentaire et des échelles temporelles de la réponse du fond ont été calculées et calibrées à l'aide d'observations en laboratoire et in situ.

1. Introduction

In the coastal zones of many large bodies of water one finds interesting structures in sandy beds. Among the more common are varieties of near-shore sand bars. In many cases it seems that such bars are formed in response to the ambient wave regime to which the bottom is subjected.

In the present work sand bars are considered to be formed by wind generated surface gravity waves and swell. Such waves interact with beds of loose sediment, changing the bottom configuration which in turn change the way waves deform. Thus the entire system in view, comprising both the fluid and the bed surfaces, admits the possibility of complex self-interaction.

A model description of this system that applies in the case of normally incident progressive waves has been derived and is reported in earlier work (Boczar-Karakiewicz and Bona 1981; Boczar-Karakiewicz, Bona and Cohen, to appear). In this primary model the description of the sediment movement in the bed boundary layer was kept as simple as possible to provide a clear illustration of principles. This simple model when tested against the outcome of controlled laboratory experiments has already shown a good agreement with observations (Boczar-Karakiewicz, Bona and Cohen, to appear). In several quite disparate field situations, e.g. the Baltic Sea, Black Sea and Lake Michigan (Boczar-Karakiewicz and Bona 1981) the St. Lawrence Estuary (Boczar-Karakiewicz et al. 1982), and the Nedland Islands (Boczar-Karakiewicz et al. 1983), important global aspects of the bar structures have been predicted with reasonable accuracy in spite of the very considerable restriction the model used places on the sediment regime. Main outlines of the general model are presented in Section 2 for introducing results of two more sophisticated sediment movement descriptions in the bed boundary layer (Section 3). Subsequently the new modified model versions provide explicit sediment transport rates expressed in mean sediment and wave characteristics, local topography gradients and bed roughness.

At present, effort is concentrated on comparisons of these alternative and basically different approaches and results in order to calibrate more precisely the model predictions of quantities of sediment transported by waves, related bed deformations and time scales in which longshore bars are formed or modified. In the calibration procedure measurable changes in the bed topography, e.g. sand bar amplitudes, changes in bar location and the time duration of these events are compared with corresponding model predictions. In Section 4 results of such calibration based on laboratory observations are presented. Results of field measurements are also discussed and conclusions are formulated in Section 5.

2. The mathematical model

In attempting to model wave-bottom interaction where temporal variation is allowed of both free surfaces, two time scales were selected for the description of the system in view. One scale for the evolution of individual waves, and another for the development of the bed. This assumption is based on observations in laboratory scales (the flume was 0.5 m wide, 21 m long, the water depth typically 0.3 m and the wavemaker period was usually about 1.8 seconds; Boczar-Karakiewicz et al. 1981) where waves deform in seconds whereas the bed experiences significant alteration only over periods of hours. Therefore the modelling could have been approached in two consecutive stages: in the first stage the bed appears to be fixed from the view point of an individual wave, in the second the bed is allowed to change its configuration. A simple but sensibly accurate description of the wave could be derived for a configuration of the bed fixed in time but spatially variable. The nonlinear, dispersive, shallow-water theory has been used later somewhat simplified by the modal decomposition of the surface wave. It also is assumed that the waves will be completely dissipated in the very near-shore region. Still considering the bottom configuration as fixed and known the view

is taken that the layer of fluid near the bottom is viscous and sediment-laden, driven by the horizontal velocities at the bottom of the inviscid water body. Now the sediment movement in the boundary layer is analyzed. Transport rates are estimated using the mass transport velocity and assuming simply the sediment concentration to be constant.

At the second stage of modelling the longer time variable is introduced to describe the waves' cumulative effect on the bottom. The temporal bed deformations are identified with the differential movement of the sediment within the lower layer of the fluid. The bed topography is then derived via a continuity equation.

This description leads to a coupled system of non-linear evolution equations whose dependent variables are the amplitudes of both the surface wave elevation and the depth averaged velocity, and the water depth. For the purpose of comparison with typical laboratory and field data, numerical integrations are accomplished using a stable fourth-order accurate predictor-corrector scheme.

In summary, the model suggested here has the general form

$$\frac{\partial a_1}{\partial X} = A_1(a_1, a_2, h) \tag{2.1}$$

$$\frac{\partial a_2}{\partial X} = A_2(a_1, a_2, h) \tag{2.2}$$

$$\frac{\partial h}{\partial T^*} = H^*(a_1, a_2, h)$$

where the functions A_1 and A_2 describe how the local bed topography and the non-linear energy flux among the components of the wave modify local wave amplitudes a_j $(j=1,2)$. Equation (2.2) describes slow temporal changes in the bed topography due to waves, known from the solution of (2.1).

The system (2.1) and (2.2) is supplemented by auxiliary conditions,

$$a_1(0, \tau) = a_1^0$$

$$a_2(0, \tau) = a_2^0 \tag{2.3}$$

for $T^* \geq 0$, corresponding to a fixed incoming deep-water wavetrain and by a given initial bed profile

$$h(X, 0) = h^0(X). \tag{2.4}$$

All variables are non-dimensional and scaled, according to the formulae,

$$(x, z, h) = (\bar{x}, \bar{z}, \bar{h})\,\frac{1}{H}$$

$$t = \bar{t}\,\sqrt{\frac{g}{H}}$$

$$z = \bar{z}\,\frac{1}{\alpha H} \tag{2.5}$$

$$q = \bar{q}\,\frac{1}{\alpha\sqrt{gH}}\,; \qquad q = \frac{1}{H+z}\int_{-h}^{z} u\,d\bar{z}$$

$$p = \bar{p}\,\frac{1}{\rho g H}$$

where H is a characteristic depth, g is the acceleration due to gravity, $\alpha = \frac{a}{H}$, where a is the wave amplitude, and barred variables are dimensional and unscaled.

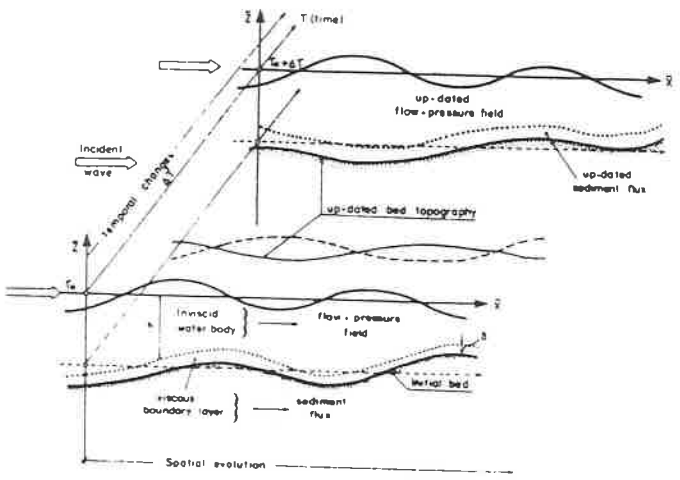

Figure 1. Scheme of the model.

The spatial and temporal coordinates are shown in Fig. 1 and the free surface elevation ζ is represented by the following truncated expansion into harmonics

$$\zeta = \zeta(x, \underline{X}, t) = \sum_{i=1}^{2} a_j(X) \exp\left[i(w_j t - k_j x)\right] + c.c. \qquad (2.6)$$

where c.c. denotes the sum of the complex conjugate of the other two summands. Here $X = \beta x$, where $\beta = \frac{H}{L}$, is an another independant horizontal spatial variable, w_1 is the frequency of the incident wave-train, $w_2 = 2w_1$ is its second harmonic and k_1 and k_2 are determined from w_1 and w_2, respectively, from the linearized dispersion relation.

With the wave component amplitudes known from (2.1), it is possible to infer the fluid velocity of the inviscid flow field. Defining u_b to be the horizontal component of the fluid velocity at $z = -h(X)$, then,

$$u_b(X,t) = \sum_{j=1}^{2} \frac{w_j}{k_j}\left[1 - \frac{1}{6}\beta^2 h^2(X) k_j^2\right] a_j(X) \exp\left[i(w_j t - k_j x)\right] + c.c \qquad (2.7)$$

With u_b in hand, the mass-transport velocity, u_m, may be calculated (Longuet-Higgins 1953; Boczar-Karakiewicz, Bona and Cohen, to appear)

$$u_m(X,z) = \sum_{j=1}^{2} \frac{w_j}{k_j}\left[a_j(X)\right]^2\left[1 - \frac{\beta^2}{6} h^2(X) k_j^2\right]^2 D_j(\delta) \qquad (2.8)$$

with a vertical depth distribution

$$D_j(\delta) = 5 - 8\, e^{-\mu_j}\cos\mu_j + 3\, e^{-2\mu_j}\ ;\ \mu_j = \frac{\beta w_j}{2\delta} z$$

where δ denotes the boundary layer thickness $\delta = \frac{\bar{\delta}}{H}$.

Define C(z) the sediment concentration in the lower fluid layer. (For simplicity, C is taken to be identically zero outside the lower layer). The present assumption is to take the concentration to be constant and the sediment to follow the fluid motion.

The total sediment flux in the boundary layer across the point X at time T*, Q* = Q*(X,T), may now be expressed as follows,

$$Q^* = \kappa^* \int_0^{\delta} \frac{C(z')}{C_0}\, u_m\, dz' \qquad (2.9)$$

where C_0 denotes a reference concentration just above the compact bed and $\kappa^*$is a proportionality factor assumed to be constant.

When C(z') is constant the scaled quantity $\frac{C}{C_0}$ may be integrated into the factor κ.

The sediment transport rate becomes simply

$$Q = \kappa \int_0^{\delta} u_m\, dz' \qquad (2.10)$$

with z' = z-h.

The instantaneous mass balance equation given by (2.1) may be rewritten taking into account (2.10) as

$$\frac{\partial h}{\partial T^*} = \kappa \frac{\partial Q}{\partial X} \qquad (2.11)$$

The proportionality factor in (2.9) - (2.11) incorporates the influence of sediment characteristics on Q, h and on the time scale T* in which the bed topography will be deformed.

As the mass-transport velocity is a second order quantity in α, time-averaged over a wave period, the long time scale unit T* may be expressed in terms of the non-dimensional time t as follows

$$T^* = O(\alpha^{-2}\beta^{-2}) \cdot t \qquad (2.12)$$

which shows that for typical wave conditions ($\alpha = 0.1$; $\beta = 0.1$) a unity in T^* is at least 10^4 times longer than a unity of t (assuming $\cdot$ to be an O(1) quantity).

Results of calculations performed using the primary model for chosen incident wave conditions ($\alpha = \beta = 0.1$) are presented in Fig. 2. Both surfaces represent the evolution of waves and the bed from an initially horizontal topography to a barred configuration.

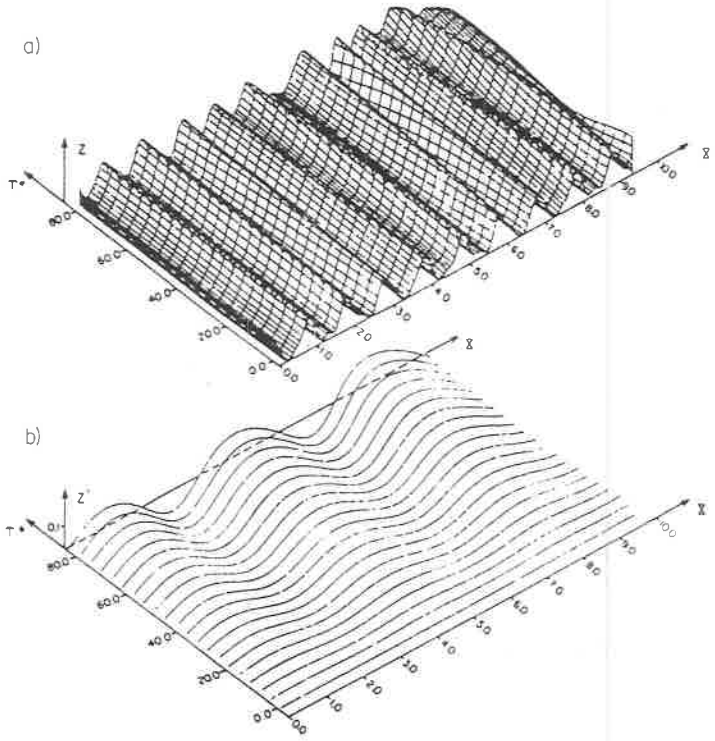

Figure 2. Evolution of waves (a) and bed topography (b) in {X, T*}.

For more precision in estimating transport rates Q and the time scale relation (2.12) two more detailed models of sediment flow in the boundary layer will be presented in Section 3.

3. Sediment transport models in the bed boundary layer

3.1 Sediment transport rates due to local flow and bed topography conditions

The general model presented in Section 2 will now be modified by an explicit sediment concentration relation and a local boundary layer thickness. The essential part of the model, as presented in Section 2, provides the expression (2.7) for the horizontal fluid velocity u_b above the boundary layer. There are number of ways to infer an associated distribution of sediment concentration. In the present work, an exponential form is considered adapted from Drew (1979). (This does not exhaust the possibilities in this aspect of modelling; see e.g. Fig. 3 after Boczar-Karakiewicz and Chapalain 1984).

According to Drew's theory, the local concentration at the time T^*, is

$$C(n, X; T^*) = C_0(X, n_0; T^*) \exp\left[\gamma(x; T^*)(n-n_0)\right] \qquad (3.1)$$

with $$\gamma = \frac{\delta_1 S}{\tau_{max}\sqrt{1+h_x^2}} \quad \text{and} \quad S = \frac{\rho_s - \rho}{\rho_s} \ , \qquad (3.2)$$

where $n = \frac{z'}{\delta}$, ρ and ρ_s denote the fluid and sediment densities, h_x the local slope of the bed and τ_{max} the maximal value of the bed shear stress during a wave period.

The reference concentration $C_0(X, n_0; T^*)$ in (3.1) can be evaluated as proposed by Smith and McLean (1977) in the form,

$$C_0(X, n_0; T^*) = C_p \frac{\gamma_0 S_t}{(1+\gamma_0)S_t} \qquad (3.3)$$

where C_p denotes the compact bed concentration, and γ_0 is an experimental constant. Here S_t is the normalized excess of shear stress on the bed

$$S_t = \frac{\psi'}{\psi_c} - 1 \ , \qquad (3.4)$$

where ψ' is the skin friction component of the Shield's parameter, and ψ_c the critical Shield's parameter (cf. Madsen and Grant 1976, Grant and Glenn 1983).

The local boundary layer thickness $\delta(X; T^*)$ and the local friction factor $f_w(X; T^*)$ may now be evaluated using Jonsson's friction diagram (Jonsson and Carlsen 1976, Jonsson 1978). The local bed roughness $k_b(X; T^*)$ due to the presence of small scale bed forms (ripples) and to additional effects caused by the moving sediment can be calculated using a relation proposed by Grant and Madsen (1982).

Once f_w is in hand the local bed shear stress can now be estimated from the maximum value of the velocity u_{bm} of the velocity u_b at the top of the boundary layer, by the formula,

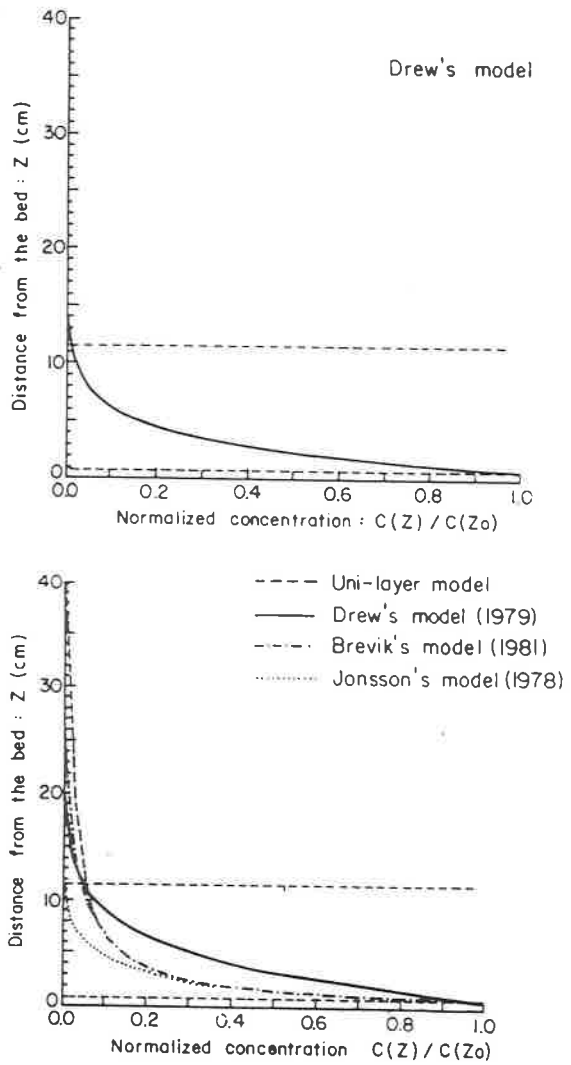

Figure 3. Sediment concentration in the bed boundary layer: a) adapted model, b) comparison of several model propositions.

$$\tau_{max}\,(X;\,T^*) = \frac{1}{2}\,f_w\,(X;\,T^*)\cdot u_{bm}\,(a_j,\,X;\,T^*)\quad . \tag{3.5}$$

The shear stress and the sediment concentration both depend on local changes in the wave field and on its asymmetry due to gradual, spatial changes in the bed topography.

The sediment concentration (3.1) leads via (2.9) to another version of the transport rates and to more precision in estimating the long time scale T*.

Considering the order of magnitude of the main boundary layer characteristics we can show the boundary layer thickness to be directly related with the wave amplitude

$$\delta \sim O(\alpha)\ .$$

The bed shear stress depends on both wave characteristics

$$\tau_{max} \approx \frac{1}{2}\,f_w\,(2\pi)^2\,\alpha^2\beta^2$$

and the reference concentration may be estimated as follows

$$\frac{C_0}{\gamma_0} \sim \tau_{max}\ .$$

Incorporating the constant γ_0 into the proportionality factor κ the sediment concentration above the bed is

$$C_0 \sim 10^2\,\alpha^2\beta^2\ . \tag{3.6}$$

Thus for typical wave conditions (α = 0.05–0.1; β = 0.1) the sediment concentration is of order

$$C_0 \sim 10^{-2} - 10^{-3}\ .$$

The latter result is in good agreement with field observations reported e.g. by Nielsen (1978). Corresponding sediment transport rates may be estimated according to (2.9)

$$Q^* \sim \kappa^*\,10^{-3}\,\alpha^2\beta \tag{3.7}$$

and the related time scale of the bed deformation is approximately

$$T^* \sim \kappa^*\,10^{-3}\,\alpha^2\beta\,\frac{\bar{t}}{T} \tag{3.8}$$

Notice that the proportionality factor κ^* in (3.7) and (3.8) still needs to be estimated.

3.2 Sediment transport rates related to the local «power» of the boundary layer flow

Bagnold (1963) related sediment transport rates to the «available power» of the boundary layer flow through constant «efficiency» factors. Bowen (1980) simplified Bagnold's formulae replacing the cubic velocity term u_b^3 by a truncated power series. Introducing into the Bagnold-Bowen's result the description of the non-linear dispersive wave of the upper,

inviscid water body (Section 2) the time averaged sediment transport rates for bed load $\overline{i_b}$ and suspended load $\overline{i_s}$, are, respectively,

$$\overline{i_b} = \frac{\frac{1}{2} f_w}{\tan \Phi} \varepsilon_b \alpha^3 Q_b \tag{3.9}$$

$$\overline{i_s} = \frac{\frac{1}{2} f_w}{w} \varepsilon_s \alpha^4 Q_s \tag{3.10}$$

with f_w - Jonsson's friction coefficient

$\tan \Phi$ - grain friction factor; ($\tan \Phi = 0.6$ a typical value for medium size sand)

w - non-dimensionalized and sacled fall velocity; $w = \frac{\bar{w}}{\alpha \sqrt{gH}}$,

$\bar{w}$ - the physical fall velocity

ε_b - bed load «efficiency» factor

ε_s - suspended load «efficiency» factor

The symbols in (3.9) and (3.10) are expressed in variables introduced in Section 2. Both denote non-dimensional quantities of O(10). (For more details see Boczar-Karakiewicz and Tessier 1984). Thus, according to Bagnold the ratio of suspended load to the bed load is a quantity of $O(\alpha^2)$. Therefore in the following derivation the contribution of suspended load will be neglected. A further step that simplifies that model is the neglect of the mass transport term in Q_b which is relatively small in comparison to the remaining two terms (the ratio are of order $\alpha\beta$). Finally the simplified model takes into account the following quantity Q_b^s of sediment transported by waves,

$$Q_b^s = u_1^2 \frac{1}{h^3} \left(\frac{3}{4} u_2 \cos \theta - \alpha \frac{4}{3\pi} u_1 \frac{h_x}{\tan \Phi}\right) \tag{3.11}$$

where θ denotes the difference of the phase of the harmonic components (note that $\theta = \theta(X)$), u_2 and u_1 are the time averaged amplitudes of the harmonic components of the velocity u_b (Section 2), and h_x denotes the local slope of the bed.

The corresponding, time averaged sediment rate which has to be introduced into the continuity equation (2.11) is

$$Q^* = \varepsilon_b \frac{\frac{1}{2} f_w}{S \tan \Phi} \alpha^3 \beta Q_b^s = \varepsilon_b S_E \alpha^3 \beta Q_b^s \tag{3.12}$$

The sediment constants and boundary layer flow characteristics are now incorporated into the constant S_E. The remaining part of the proportionality factor, ε_b, denotes Bagnold's «efficiency factor». It will appear from results presented in Section 4 that ε_b may be scale-dependent.

Estimating the order of magnitude of Q^* for a typical sediment (medium size sand) and for typical wave conditions ($\alpha = \beta = 0.1$) one obtaines

$$Q^* \cong 10^{-4} Q_b^s \tag{3.13}$$

which result is suprisingly close to that obtained in the previous model described in Section 3.1.

Similarly for the long time variables T^* one has

$$T^* = \varepsilon_b S_E \alpha^{-1} \beta^{-1} \frac{\bar{t}}{T}. \tag{3.14}$$

Returning to the expression (3.11) it is visible that in Bagnold's model the sediment flux may be reversed when the local gravity force dominates the wave induced force, i.e. when

$$h_x > \frac{1}{\alpha} \frac{9\pi}{16 \tan \Phi} \frac{u_2 \cos \theta}{u_1} \tag{3.15}$$

4. On the calibration of model predictions: the time scale of bed deformation

For the sediment models developed in Section 2 and 3, the predicted transport rate Q^* and the relative time scales of bed and wave deformations, T^* and t, respectively, can be

$$Q^* = \frac{\bar{Q}}{H \sqrt{gH}} = \kappa^* S_E \alpha^n \beta^m \cdot Q \tag{4.1}$$

$$t = \frac{\bar{t} \sqrt{g}}{\sqrt{H}} = \frac{1}{\alpha^n \beta^m} \frac{1}{\kappa^*} \frac{1}{S_E} T^* \tag{4.2}$$

where $\bar{Q}$ is expressed in physical variables of sediment transported by the waves, T^* denotes the unit of the long time scale, and n, m, κ^* and S_E are all constants defined in Section 2 and 3. These constants are estimated for the three sediment models as shown in Table 1.

TABLE 1

Boundary layer model \ Relevant constants	κ^*	S_E	n	m
(1) Constant sediment concentration	non-specified	non-specified	2	2
(2) Local sediment & boundary layer characteristics	non-specified	$\sim 10^{-3}$	2	2
(3) Bagnold's «energetic» description	$\varepsilon_b \cong 10^{-1}$	$\frac{1/2\ f_w}{\tan \Phi} \cong 10^{-1}$	3	2

If, as is often practical, time is counted, in wave periods, then (4.1) and (4.2) become,

$$\frac{\bar{t}}{T} = \frac{1}{\kappa^*} \frac{1}{S_E} \frac{1}{\alpha^2 \beta} T^* \quad , \tag{4.3}$$

$$Q^* = \frac{\bar{Q}}{H^2 T^{-1}} = \kappa^* S_E \alpha^2 Q \quad . \tag{4.4}$$

An explicit proportionality factor κ_E can be introduced according to Bagnold's model version (see Table 1)

$$\kappa_E = \frac{\frac{1}{2} f_w \epsilon_b}{\tan \Phi} \alpha \tag{4.5}$$

The order of magnitude of κ_E for typical wave and sediment conditions is

$$\kappa_E = O(10^{-3}) \tag{4.6}$$

with this value of κ_E the expressions (4.1) and (4.2) are identical to those proposed in the simple model in Section 2.

The results reported above need now to be compared with observations. Both the transport rate and the time scale are naturally interrelated through the proportionality factor κ_E. However, measurements of local values of Q are complex even in laboratory situations. Therefore we have chosen to determine κ_E calibrating the time scale over which bars form.

In the first prototypical example sand bars were formed by waves in a laboratory flume (Boczar-Karakiewicz et al. 1981). In all experiments the mean initial water depth is constant. The formation of a two-bar system from an initially horizontal bed is shown in Fig. 4. Similar experiments were set up simulating the modification of a bar system by a wave having different parameters and simulating the migration of bars due to slow, non-periodic changes in the mean water level.

The comparison of calculations (Fig. 2) and measurements (Fig. 4) showed the proportionality factor κ_E to be a quantity of $O(10^{-1})$, thus, about 100 times larger than predicted by (4.6). Calibrations showed also that changes in bar configurations due to a new wave and depth regime occured in time scales similar to those bars were generated.

For further investigations, we have chosen an example in a natural environment with larger typical horizontal scales, but which is still relatively well controlled. On Lake Michigan observations has shown the system of bars to be shifted landward about 100 meters during a period of two years (Saylor and Hands 1972). Changes in the bar system were caused by a slow rise in the mean water level of about 1.0 m. The estimate of the corresponding proportionality factor κ_E shows to be of order $O(10^{-2})$. This result provides κ_E to be 10 times smaller than the value obtained in laboratory, but still not as low as predicted by (4.6). A value of κ_E of order 10^{-2} was also obtained from observations from the Georgian Bay of Lake Huron (Greenwood and Sherman 1984; Davidson-Arnott and Randall 1984). It is worth a special note that bar systems do not

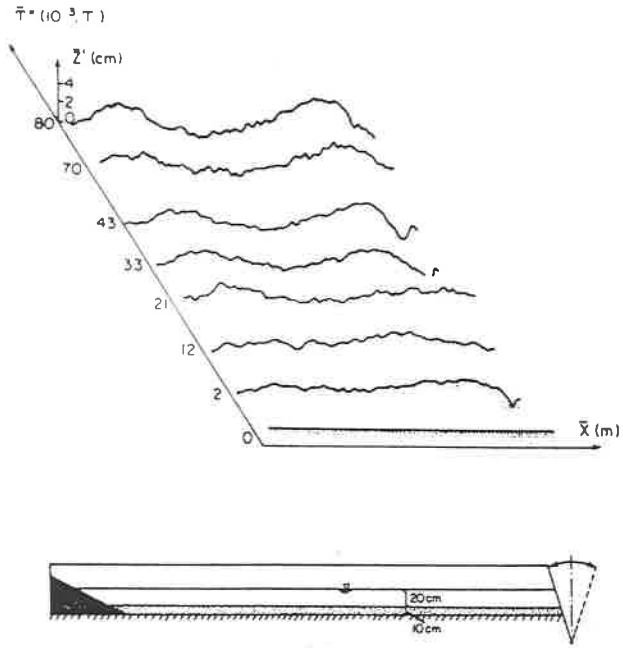

Figure 4. Formation of sand bars in a laboratory experiment: wave period T = 1.84 s.

change their essential topography during a relatively short event such as a single storm (see at Figure 5). The same quantitative result has been obtained in our numerical experiment.

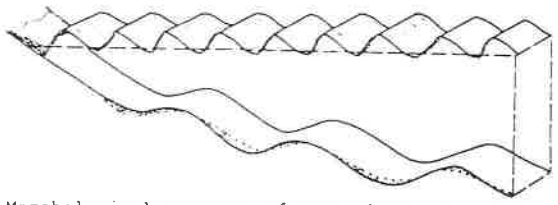

Figure 5. Morphological response of near shore bars at Wendake Beach inferred from measurements (31-05-1980-01-06-1980). Cross-hatching represents areas of erosion, dots areas of accretion A solid line indicates the post-storm profile (after Greenwood and Sherman 1984).

5. Discussion

This report has been concerned with technical issues regarding simple wave-bottom interaction models for the formation, modification and displacement of wave-generated bar structures in shallow water. Such models have been shown to be effective over a fearly wide range of scales, so justify a more detailed study of their properties. The results reported here on the calibration of such models represent a preliminary stage of an ongoing investigation. The use of two time scales for this sort of problem seemes to be well justified. Even on laboratory scales, the bed deformed in time intervals of order 10^3 when compared to the wave period.

References

Bagnold, R.A. 1963. Beach and nearshore processes. Part I : Mechanics of marine sedimentation. Contribution to: The Sea, vol. 3, General editor: M.N. Hill. pp. 507-528.

Boczar-Karakiewicz, B., B. Paplinska and J. Paplinska and J. Winiecki. 1981. Formation of sand bars by surface waves in shallow water laboratory experiments. Rozprawy Hydrotechniczne, 41 : 111-125.

Boczar-Karakiewicz, B. and J.L. Bona. 1981. Formation of sand bars on sandy beaches by progressive waves. Mitteilungen des Leichtwei8 - Instituts für Wasserbau Tech. Univ. Braunschweig, pp. 378-420.

Boczar-Karakiewicz, B., J.L. Bona and D.L. Cohen (to be submitted). Interaction of shallow-water waves with a bottom topography. Journal of Physical Oceanography.

Boczar-Karakiewicz, B. and G. Chapalain. 1984. Model of sediment transport by shallow water waves in a turbulent boundary layer. Internal Report, INRS-Océanologie, 84 p.

Boczar-Karakiewicz, B., G. Drapeau and B.F. Long. 1984. Modélisation des barres sableuses littorales de la partie nord des Iles-de-la-Madeleine. Sciences et Techniques de l'Eau, 17 (1) : 35-39.

Boczar-Karakiewicz, B., B.F. Long and G. Drapeau. 1983. Formation and modification of a system of sand bars by progressive gravity waves in the presence of tides (an example from the North Coast of the Gulf of St. Lawrence). Proc. of the Canadian Coastal Conference, Vancouver, pp. 37-51.

Boczar-Karakiewicz, B. and B. Tessier. 1984. Simple model of nearshore sedimentation by shallow water waves: beach stability and longshore bars. Internal Report, INRS-Océanologie, 36 p.

Bowen, A.J. 1980. Simple models of nearshore sedimentation; Beach profiles and longshore bars. In: The coastline of Canada, S.B. McCann (Editor), pp. 1-11.

Brevik, I. 1981. Oscillatory rough turbulent boundary layers. Journal of Waterway, Port, Coastal and Ocean Division, ASCE, 107 (WW3) : 175-188.

Davidson-Arnott, R.G.D. and D.C. Randall. 1984. Spatial and temporal variations in spectra of storm across a barred nearshore. Mar. Geol., 60 : 15-30.

Drew, D.A. 1979. Dynamic model for channel bed erosion. Journal of the Hydraulics Division, ASCE, 6 : 721-736.

Grant, W.D. and S.M. Glenn. 1983. Continental shelf bottom boundary layer model, vol. 1: theoretical model development. Woods Hole Oceanographic Institution, 163 p.

Grant, W.D. and O.S. Madsen. 1982. Movable bed roughness in unsteady oscillatory flow. Journal of Geophysical Research, 87 (C1) : 469-481.

Greenwood, B. and D.J. Sherman. 1984. Waves, currents, sediment flux and morphological response in a barred nearshore system. Mar. Geol. 60 : 31-61.

Jonsson, I.G. 1978. A new approach to oscillatory rough turbulent boundary layers. Technical University of Denmark, Inst. of Hydrodynamics and Hydraulic Engineering, Ser. Pap. 17, 87 p.

Jonsson, I.G. and N.A. Carlsen. 1976. Experimental and theoretical investigations in an oscillatory turbulent boundary layer. Journal of Hydraul. Res., 14 : 45-60.

Longuet-Higgins, M.S. 1953. Mass transport in water waves. Phil. Trans. Roy. Soc., London, A, 245 : 535-591.

Madsen, O.S. and W.D. Grant. 1976. Qualitative description of sediment transport by waves. Proc. of the 15th Coastal Engineering Conference, ASCE, pp. 1093-1112.

Nielsen, P. 1979. Some basic concepts of wave sediment transport. Technical University of Denmark, Inst. of Hydrodynamics and Hydraulic Engineering. Ser. Pap. 10, 160 p.

Saylor, J.H. and E.B. Hands. 1970. Properties of longshore bars in the Great Lakes. Proc. of the 12th Coastal Engineering Conference, ASCE, pp. 839-853.

Smith, J.D. and S.R. McLean. 1977. Spatially averaged flow over a wavy surface. Journal of Geophysical Research, 82 (2) : 1735-1746.